UNIVERSITY OF LEEDS

This is a repository copy of *Water transport facilitated by carbon nanotubes enables a hygroresponsive actuator with negative hydrotaxis*.

White Rose Research Online URL for this paper:
http://eprints.whiterose.ac.uk/158026/

Version: Accepted Version

Article:
Chen, H, Ge, Y, Ye, S orcid.org/0000-0001-5152-5753 et al. (6 more authors) (2020) Water transport facilitated by carbon nanotubes enables a hygroresponsive actuator with negative hydrotaxis. Nanoscale, 12 (10). pp. 6104-6110. ISSN 2040-3364

https://doi.org/10.1039/d0nr00932f

© The Royal Society of Chemistry 2020. This is an author produced version of a journal article published in Nanoscale. Uploaded in accordance with the publisher's self-archiving policy.

Reuse
Items deposited in White Rose Research Online are protected by copyright, with all rights reserved unless indicated otherwise. They may be downloaded and/or printed for private study, or other acts as permitted by national copyright laws. The publisher or other rights holders may allow further reproduction and re-use of the full text version. This is indicated by the licence information on the White Rose Research Online record for the item.

Takedown
If you consider content in White Rose Research Online to be in breach of UK law, please notify us by emailing eprints@whiterose.ac.uk including the URL of the record and the reason for the withdrawal request.

White Rose university consortium
Universities of Leeds, Sheffield & York

eprints@whiterose.ac.uk
https://eprints.whiterose.ac.uk/

Check for updates

View Article Online
View Journal

Nanoscale

Accepted Manuscript

This article can be cited before page numbers have been issued, to do this please use: X. Yang, H. Chen, Y. Ge, S. Ye, Z. Zhu, Y. Tu, D. Ge, Z. Xu and W. Chen, *Nanoscale*, 2020, DOI: 10.1039/D0NR00932F.

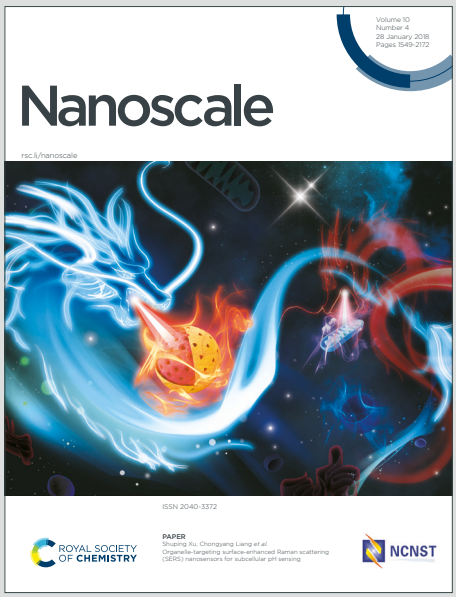

This is an Accepted Manuscript, which has been through the Royal Society of Chemistry peer review process and has been accepted for publication.

Accepted Manuscripts are published online shortly after acceptance, before technical editing, formatting and proof reading. Using this free service, authors can make their results available to the community, in citable form, before we publish the edited article. We will replace this Accepted Manuscript with the edited and formatted Advance Article as soon as it is available.

You can find more information about Accepted Manuscripts in the Information for Authors.

Please note that technical editing may introduce minor changes to the text and/or graphics, which may alter content. The journal's standard Terms & Conditions and the Ethical guidelines still apply. In no event shall the Royal Society of Chemistry be held responsible for any errors or omissions in this Accepted Manuscript or any consequences arising from the use of any information it contains.

ROYAL SOCIETY OF CHEMISTRY

rsc.li/nanoscale

Please do not adjust margins

View Article Online
DOI: 10.1039/D0NR00932F

Journal Name

ARTICLE

The water transport facilitated by carbon nanotubes enables a hygroresponsive actuator with a negative hydrotaxis

Received 00th January 20xx,
Accepted 00th January 20xx

DOI: 10.1002/x0xx00000x

www.rsc.org/

Hui Chen, ‡[a] Yuanhang Ge, ‡[a] Sunjie Ye,[d] Zhifeng Zhu,[a] Yingfeng Tu,[a] Denteng Ge,[e] Zhao Xu,[e] Wei Chen[c] and Xiaoming Yang*[ab]*

Hygroresponsive actuators harness minor fluctuations in the ambient humidity to realize energy harvesting and conversion, thus of profound significance towards more energy-saving and sustainable systems. However, most of existing hygroresponsive actuators are only adaptive to wet environment with limited moving directions and shape morphing modes. Therefore, it is highly imperative to develop hydroresponsive actuator that works in both wet and dry environments. In this work, we present a bidirectinal actuator responsive to both wet and dry stimuli. Our strategy relies on the introduction of carbon nanotubes to provide tranport channels of water molecules. The actuation is enabled by the rapid transport of water in and out of the system driven by the moist/dry surroundings owing to the transport channels. The resultant actuator demonstrates reconfiguration and locomotion with turnover frequency of F=30 min^{-1}, coupled with the capability of lifting objects 6 times heavier and transporting cargos 63 times heavier than itself. Oscillations (24°) driven by dry air flow in a cantilever dipsplay a high frequency (2 Hz) and large amplitude. Furthermore, a touchless electronic device was constructed to output varying signals in response to humid and dry environment. Our work provides valuable guidance and implications for designing and constructing hygroresponsive actuators, and paves the way to the next-generation robust autonomous devices to exploit the energy from natural resources.

Introduction

Hygroresponsive actuators are capable of translating the energy contained in the water/moisture/humidity into mechanical work, and hold potential for contributing to tackling the global energy crisis by taking advantage of the energy in the natural environment.[1] Inspired by various hygroresponsive natural organisms, such as pinecones that close under a wet condition and open when drying out, many hygroresponsive biomimetic actuators have been fabricated.[1-13] Materials studied in hydroresponsive actuators are usually hydroexpansive materials either artificial or natural including carbon nitride,[14] cellulose nanofiber,[15,16] Polypyrrole,[17] graphene,[18] polydopamine,[19] silk,[20] polyelectrolyte multilayer,[21] liquid crystal, [22, 23] commercial perfluorosulfonic acid ionomer (PFSA) film,[24] natural alginate[25] and so on. Many previously studies demonstrated hygroscopic actuators move when humidity is raised either by external supply of water vapor or by being placed near a water source. However, little attention was paid to the performance of actuators when the humidity of environment is decreased, which limiting their scale of deformation and scope of applications. The development of actuators workable under both dry and wet conditions is rare and urgently needed. The challenge for achieving this goal lies in the judicious material design of the molecular composition, intermolecular interactions and microstructures.

In light of reported research on hygroresponsive actuators,[26-28] as well as our previous work on homogeneous graphene oxide actuator which shows fast response to moisture,[29] we found that materials with strong hydrophilicity such as hydrophilic polymers exhibit excessively rapid water adsorptions but slow water desorption due to strong hydrogen bonding interactions between polymer chains and water molecules. These features may lead to a deflection-relaxation response, which causes low recovery speed and inactivity in dry environments.[30,31] We expect that the introduction of nano-channels for water transport can facilitate water flow permeability, eventually enables the rapid response of the actuator to both wet and dry stimuli. To this end, multiwall carbon nanotubes (MWCNTs) represent an ideal candidate material. It is reported that MWCNTs

[a] State and Local Joint Engineering Laboratory for Novel Functional Polymeric Materials, Suzhou Key Laboratory of Macromolecular Design and Precision Synthesis, Jiangsu Key Laboratory of Advanced Functional Polymer Design and Application, Department of Polymer Science and Engineering, College of Chemistry, Chemical Engineering and Materials Science, Soochow University, Suzhou 215123,P. R. China. E-mail: yangxiaoming@suda.edu.cn.
[b] State Key Laboratory of Pollution Control and Resource Reuse, School of the Environment, Nanjing University, Nanjing 210023, PR China.
[c] Research Centre for Smart Wearable Technology, Institute of Textiles and Clothing, The Hong Kong Polytechnic University, Hong Kong 999077, P. R. China. E-mail: weii.chen@polyu.edu.hk
[d] School of Physics and Astronomy, University of Leeds, LS2 9JT, Leeds, UK.
[e] State Key Laboratory of Advanced Textile Materials and Manufacturing Technology (Zhejiang Sci-Tech University), Ministry of Education. State Key Laboratory for Modification of Chemical Fibers and Polymer Materials Institute of Functional Materials, Donghua University, Shanghai 201620, P. R. China.

† Footnotes relating to the title and/or authors should appear here.
Electronic Supplementary Information (ESI) available: [details of any supplementary information available should be included here]. See DOI: 10.1002/x0xx00000x.
‡ These two authors contributed equally to this work.

Published on 24 February 2020. Downloaded by University of Leeds on 2/27/2020 8:47:54 PM.

Nanoscale Accepted Manuscript

Please do not adjust margins

View Article Online DOI: 10.1039/D0NR00335

Published on 24 February 2020. Downloaded by University of Leeds on 2/27/2020 8:47:54 PM.

possess hydrophobic nano-channels for confining water molecules into single-file conformation to attain an ultra-fast flow velocity.[32-35]

In this study, we have fabricated a hygroresponsive actuator via the incorporation of multiwall carbon nanotubes (MWCNTs) with chitosan (CS), a naturally occurring polysaccharide. MWCNTs provide transport channel for water molecules to move in and out, while CS is hydroexpansive material. Upon the exposure to the moist stimulus from one side, the film harnesses the humidity for generating rapid and non-uniform exchange of water with the environment to undergo swelling to show a series of mechanical actuation movements. Intriguingly, the exposure of the film to dry stimulus leads to the contraction of the composite film via the desorption of water and the motion in the reversed direction, thereby conferring the capability for bidirectional actuation and fast gating of the motility triggered by wet and dry stimuli. Oscillations of high frequency (2 Hz) and large amplitude (24°) are obtained, driven by dry airflow in cantilevers due to the actuator response to both wet and dry environment. The design rationale and fabrication of a bidirectional actuator presented here will provide insightful guidance and implications for engineering novel and advanced hygroresponsive actuators.

Experimental section.

Chemicals.

CS of Viscosity > 400 mPa.s was purchased from Aladdin. It was prepared by deacetylation of chitin from crab shells and had a degree of deacetylation of 82.7%. The MWCNTs (length: 5-15 μm, diameter: 20-40 nm, purity > 95%, ash < 2%) were purchased from Shenzhen Nanotech Port Co., Ltd. The MWCNTs were further refluxed in a mixture of concentrated sulfuric acid (98%) and nitric acid (65%) with a volume ratio of 3/1 at 90 ℃ for 10 min to increase the amount of carboxylic and hydroxyl groups (with about 2.3 *wt*% weight loss, determined by thermogravimetric analysis).

Fabrication of Flexible Free-Standing Uniform CS/MWCNTs composite film.

The prepared hydrophilic MWCNTs were dispersed in distilled water (100 mL). Then the suspensions of MWCNTs were homogenized in an ultrasonic bath (JAC-Ultrasonic 1505P) for 1 h. 1.0 g chitosan was added to 100 mL acetic acid solution (1%). The two solutions were mixed and stirred with a mechanical homogenizer (IKA Ultra-Turres T 18) at 18 000 rpm for 30 min, followed by a 20 min-sonication for removing the bubbles. Then the CS/MWCNTs solutions were poured into a plastic culture dish (diameter = 4.5 cm) and heated at 50 °C to allow water to evaporate. The dried uniform thin films with an average thickness of 20~40 μm were easily peeled off from their supports, without the requisition of particular treatment.

Characterization.

The exact widths and the thicknesses were determined by micrometer calipers. The cross-section images of the film were collected on scanning electron microscopy (SEM, Quanta 400 FEG). The tensile tests were performed in an Instron universal material testing system (model 5567) with a gauge length of 10 mm and a crosshead speed of 5 mm/min at room temperature. Properties reported here represent the mean results for at least six specimens. The water responses of CS, MWCMTs, and composite films were monitored by using a quartz crystal microbalance (QCM, Q-Sense E4) in a humidity module. A thin layer of sample was evenly deposited on a QCM sensor coated with gold. The sensor was loaded in the humidity module. Pure water vapor (relative humidity = 100%) and indoor air (relative humidity = 50%) were flowing inside the humidity module. It is assumed that the humidity change in the chamber of the humidity module is linearly proportional to the gradual switch between pure water (100% RH) and indoor humidity (50% RH). Upon the adsorption and desorption of water, the change in the mass of each film was calculated based on the measured change in the frequency of the QCM sensor.

Testing of actuation behaviors driven by humidity gradient.

The experiments were carried out in a laboratory with the relative humidity (RH) of 50%. A circular film was placed over a piece of moist filter paper and tested at different temperatures. In a typical strip actuator system, the film was clamped at one end and exposed to moist (RH = 100%) and dry (RH = 0%) nitrogen. The distance of the stimulus to the film and the gas flow speed were both investigated to determine the optimized value (Fig. S1). The bending/unbending process and oscillation performance of composite film were recorded with a digital camera (Canon EOS 70D).

COMSOL Simulation of the Humidity Gradient.

To simulate the deformation of the film, a model of the air chamber and film was set up and analyzed by COMSOL Multiphysics method. The humidity distributions were determined with the module for moisture transport in air by neglecting air flow-induced transport. The moisture source and film were under ambient pressure, so that only the diffusion of water vapor can be supplied. The diffusion flux of water vapor in air was 2.85 kg/(m^2·s).[36] The relative humidity (RH) provided by the moist nitrogen and dry nitrogen were set to match the experimental values of the RH, which were typically 100% and 0% RH, respectively. The environmental RH was set as 30%, 50%, and 70%. The left side of the chamber was the outflow boundary, the source was a small window on the right side, and the rest was a non-permeable boundary. The film model was placed 20 mm from the moisture source in the chamber and its thickness has been exaggerated so that the film was clearly visible in the snapshots. All cross-sectional humidity distributions presented

Nanoscale Accepted Manuscript

 This journal is © The Royal Society of Chemistry 20xx

Please do not adjust margins

View Article Online

Published on 24 February 2020. Downloaded by University of Leeds on 2/27/2020 8:47:54 PM.

were obtained through thin films and moisture and dry sources located at the right boundary of chamber.

Results and Discussion

In this study, CS and MWCNTs were mixed together to form homogeneous composite film at macroscale (Fig. 1a). In a typical strip actuator system, the film clamped at one end and exposed to stimuli exhibited a bidirectional actuation behavior in response to wet and dry stimulus (Fig. 1b, Supplementary Movie 1&2). The sample bends away from the moisture source but towards the dry source. As a result, the humidity changes of the source contributed to a repeatable bending deformation in a large scale. The bending/unbending angles of composite film were investigated as a function of time and stimulus. The bending angle is defined from the angle between the linkage line and the basic line. The linkage line is formed based on the tilted end of the sample and the original end of the sample. As shown in Fig. 1c&d, the average bending speed is larger than the unbending speed in the actuation driven by both moist and dry source. The bending speed and maximum angle induced by moist source is slightly larger than that by dry source.

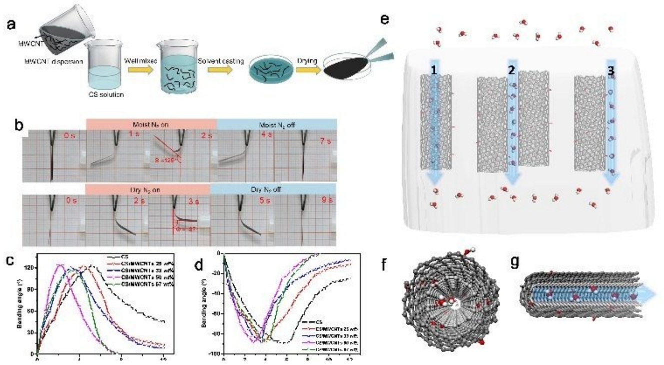

Fig. 1 (a): Schematic illustration of the preparation of CS/MWCNTs composite film; (b): Bending and unbending behavior of a strip actuator (film length = 25 mm, width = 4 mm, and thickness = 40 μm) in response to moist and dry stimuli by adsorption and desorption of water molecules (the stimulus is from the right side of the composite film); (Scale bar: 1 cm); Time-dependent angles of bending and unbending deformation of neat chitosan and its composite strips with varying contents of MWCNTs to (c) wet stimulus (RH=100%) and (d) dry stimulus (RH=0). Schematic of possible pathways for water transport facilitated by MWCNTs in a composite film (e), including: (1) ultrafast water transport through CNT interiors, owing to the chain-like structure of water molecules connected by hydrogen bonds (f&g); (2) flux enhanced by nano-confinement effect of the space between CNTs (3) local transport on hydrophobic regions of the external surface, boosted by hydrophobic effect. (In e, f&g, grey color: carbon atoms; red color: oxygen atoms; white color: hydrogen atoms).

To optimize the content of the MWCNTs for best performance, films with four weight contents of MWCNTs (25 *wt*%, 33 *wt*%, 50 *wt*% and 67 *wt*%) were prepared and tested (Fig. 1c&d). Fig. 1 c&d show the time-dependent angles of bending and unbending deformation of neat chitosan and its composite strips upon wet and dry stimuli. The pure CS film showed slow bending and recovery because of high water-adsorbing capacity[37] and strong hydrogen interaction between CS and water molecules.[38,39] In the presence of MWCNTs, the strip bent rapidly in response to the stimulus and recovered quickly after the removal of stimulus. However, with further increasing the content of MWCNTs to 67 *wt*%, the response ability was decreased, possibly due to the decreased amount of hydroexpansive chitosan chains. The hybrid film containing 50 *wt*% MWCNTs displayed optimal response performance. It is noteworthy compared with composite containing 50 *wt*% MWCNTs, the composite film with 67 *wt*% of MWCNTs showed faster recovery, under both moist and dry stimuli (Fig. 1c and d). This difference is attributable to the larger strain energy of the composite film with 67 *wt*% of MWCNTs, due to higher Young Modulus. (See ESI for details). Unless otherwise specified, the composite film studied in this work is CS/MWCNTs 50 *wt*%. In consideration of previous literatures on the water transport of carbon nanotubes (CNTs),[40-45] we ascribe this difference in the hygroresponsive actuation performance to CNTs-enhanced water transport (Fig. 1e).[46] CNTs can facilitate water transport in a polymer matrix via the following pathways: (1) ultrafast water transport through CNT interiors, owing to the chain-like structure of water molecules connected by hydrogen bonds (Fig. 1f&g); (2) flux enhanced by nano-confinement effect of the space between CNTs (3) local transport on hydrophobic regions of the external surface, boosted by hydrophobic effect. [47-50]

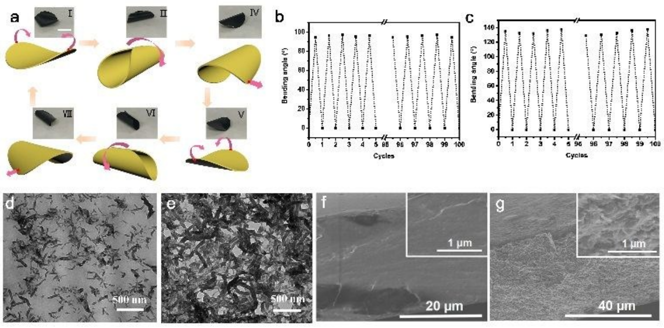

Fig. 2 (a) Flipping locomotion of a circular film (CS/MWCNTs 50*wt*%) on a moist substrate at 40 °C. (Scale bar: 1 cm). (b&c) Plots of the reversible bending/unbending behaviors of the film upon cyclic exposure to moist and dry stimulus (100 cycles without obvious fatigue). TEM images of a thin section of the CS/MWCNTs 25 *wt*% (d) and CS/MWCNTs 50 *wt*% (e). Cross-section SEM image of (f) CS and (g) the composite film (CS/MWCNTs 50 *wt*%), with inset showing the image of higher magnification.

Intriguingly, the circular composite film displays a locomotive cycle consisting of eight stages on a moist substrate (Fig. 2a and Supplementary Movie S3). After the film is placed on a moist substrate, the water adsorption-induced expansion of the film surface in contact with the substrate is superior to that of the opposite surface (in contact with air), whereby the film folds up (I) to form a tubular structure (II). As the center of gravity rises, the film topples over (III), and then the upper surface turns down (IV). Afterwards, the film bends from one corner, rolls over horizontally (V) and shapes into a tube again (VI). The mechanical instability results in the turn-over of the tube. The upper faces slides down and nearly recovers to the initial unfolded state (VIII). Owing to the asymmetric swelling arising from the in-situ formation of bi-layer structure, the film continues to roll up as a start of a new cycle. When the film was moved away from the moist filter paper, the motion of

Nanoscale Accepted Manuscript

Please do not adjust margins

View Article Online

Published on 24 February 2020. Downloaded by University of Leeds on 2/27/2020 8:47:54 PM.

the film pauses instantaneously, and can be restarted by placing the film back onto the moist paper. The temperature influences the water exchange kinetics. It is found that the film shows best performance at 40 °C in this study. At 25 °C, the kinetics of water evaporation from the moist substrate is relatively slow, decelerating the motion of the film. The higher temperature (75 °C) does not increase the rolling frequency, because the fast water adsorption at this temperature results in the formation of wet and soft film. The thickness of the film also affects the turnover frequency of the film. For a circular film (diameter = 4.5 cm) with a thickness of 20 μm, the frequency was F=30 min^{-1}. However, a small thickness gives rise to rapid deterioration (after 5 cycles). Increase of the thickness to 40 μm decreases the turnover frequency to F= 20 min^{-1}, and improves the stiffness and durability, enabling the repeated turnover without deterioration after more than 20 cycles. When the thickness of film was further increased to 60 μm, the turnover frequency decreased to F = 4 min^{-1}.

Notably, the motilities of both circular film and strip actuator are highly reversible and reproducible and can be switched on and off for more than one hundred times without obvious fatigue. Fig. 2b&c shows the bending and unbending deformations of a strip actuator, as demonstrated by a graph of the film bending angle versus time, upon the exposure to stimulus over 100 cycles with on/off switches.

This observed deformation is caused by an inhomogeneous swelling/shrinking that starts at the film side facing the source, which has more pronounced water adsorption/desorption. The mechanism of water exchange of composite (CS and MWCNTs) with environment is shown in Fig. S2. CS possesses three kinds of functional hydrophilic groups in a glucosamine unit, including amino groups, primary and secondary hydroxyl groups. The functionalized MWCNTs also contain hydrophilic carboxylic and hydroxyl groups which are capable of inducing intermolecular hydrogen bonding with water molecules (Fig. S2), bringing about good miscibility between these two components, which would facilitate actuation performance. This speculation is supported by the contact angles of MWCNTs upon varying durations of acid treatment and the actuation performance of corresponding composite film (Fig. S3 and S4). The film of MWCNTs without acid treatment is super hydrophobic, while the contact angles of MWCNT film upon acid treatment for 5 min and 10 min are respectively 160.84° and 112.34°, suggesting the acid treatment can improve the hydrophilicity of MWCNTs by increasing the number of hydrophilic groups. This improvement leads to better miscibility of MWCNTs with chitosan in the composite film which favors water transport. Eventually, the composite film containing MWCNTs upon 10 min of acid-treatment displayed optimal response and recovery performance upon wet and dry stimuli. In addition, the enhanced miscibility between MWCNTs and chitosan can also improve the mechanical properties of the composite film (Fig. S5&Tab. S1).[51]

All the samples showed fast water adsorption/desorption when the humidity was increased or decreased (Fig. 3a). Hence, we tested the adsorption capacity of the composite film. The mass of composite film increases from 0.6503 g to 0.7855 g with the water adsorption of about 20.8% (Fig. S6a), as the humidity is altered from 20% to 100%. While for CS, the water adsorption is about 53% (Fig. S6b), larger than that of the composite film. However, the adsorption speed of water molecules of composite film is faster than that of CS. It can be concluded that the presence of MWCNTs can provide the water molecule transport channel. Furthermore, a quartz crystal microbalance (QCM), a sensitive tool to detect the weight changes of the sample at nanogram scale, was used to monitor the weight changes upon the change of environment humidity. Fig. S6c shows that all the samples rapidly adsorb water molecules from humid air after the environment humidity increases from 50% to 100%, revealing the instant response of the film to water vapor. The increase in the mass of the composite film is faster than that of the film of pure chitosan or MWCNTs when the environment humidity increases from 50% to 100%, which suggests the faster water adsorption of the composite film, demonstrating MWCNTs are responsible for facilitating the water adsorption. Similarly, the mass of composite film decreases from 1.2809 g to 1.2115 g with the water desorption of about 6% (Fig. S6d), as the humidity is altered from 50% to 0. While for CS, the water desorption is about 3% (Fig. S6d), smaller than that of the composite film, which reveals that the presence of MWCNTs can also accelerate the water desorption.

The microstructure of the film also plays an important role in determining its water adsorption rate. TEM images (Fig. 2 d&e) of a thin section from the film exhibit local aggregation for CS/MWCNTs 25 *wt*%, and network structures of MWCNTs for CS/MWCNTs 50 *wt*%. Fig. 2f&g and Fig. S7 shows the cross-section SEM images of composite and CS film after tensile testing. The composite film displays porous structure while the film of CS exhibits smooth structure. It is acknowledged that porous structure endows materials with enhanced actuation performance, since it can enlarge the interfacial area of materials/air and provides increased number of water pathways during water adsorption/desorption.[31] Consequently, the equilibrium between the water in the loaded film and in the surroundings can be established quickly. This equilibrium is dynamic, and can be shifted and re-established very quickly upon the variation, leading the composite film to be highly sensitive to even very small humidity difference. The porous microstructure of the film as well as the hydrophilic group of the materials provide the possibility of the humidity-driven response of the composite film (Fig. 3a).

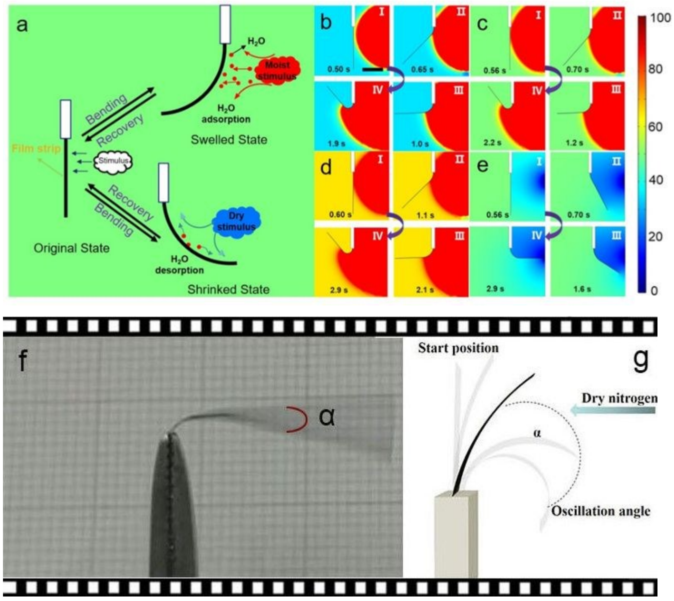

Fig. 3 (a) Schematic illustration of the mechanism of bidirectional actuation with environmental relative humidity of 50%; (b-e) Theoretical modeling of the bidirectional actuation behavior of a sample: calculated RH distributions around a strip during the bending

Nanoscale Accepted Manuscript

This journal is © The Royal Society of Chemistry 20xx

Please do not adjust margins

deformation (Film thickness was exaggerated for clarity): (b-d) Moist stimulus with environmental relative humidity of 30%, 50%, and 70%; (e) dry stimulus with environmental relative humidity of 50%. (f) Snapshot of the oscillating film. (g) The film is mounted vertically and oscillates with full oscillation angle, around the horizontal plane of the incidence of dry nitrogen.

The influences of the local environment on the film are critical for generating the observed actuation behaviors. To clearly understand the actuation of the film driven by the humidity, we simulate the environmental humidity distribution. It has been reported that the diffusion of water vapor in air is $\approx 10^7$ times faster than diffusion through the film, indicating that the humidity distribution equilibrate around the film instead of through it (Fig. 3b).[52] The dominant effect of the absence of flux through the film is to significantly amplify the ΔRH between the surface of the film exposed to stimulus and the unperturbed side. As the film responds to the stimulus, it alters its local environment driving a subsequent reconfiguration, and so on as shown in Fig. 3 b~e. Fig. 3e shows the dry stimulus (RH=0%) with local environment (RH=50%), while Fig. 3b&d show the humid stimulus (RH=100%) with different local environment (RH=30%, 50% or 70%). The larger ΔRH between two sides of the film enables more chemical potential energy to be harvested for overcoming the energetic barriers to undergo the motion.

The responses of the film to both moist and dry stimulus enable the fabrication of a cantilever that shows moisture-drive oscillation with high frequency (2 Hz) and large amplitude (24°). The oscillation of the cantilever can be triggered by the dry nitrogen flow velocity of 2 L/min, and the behavior shows little fatigue over hundreds of cycles. Fig. 3g depicts the mechanism of the observed oscillation. Upon the exposure to dry stimulus, the film side facing dry nitrogen undergoes more remarkable desorption of water molecules, giving rise to inhomogeneous shrinking of the film, which leads the film to bend towards the dry nitrogen. The moment of inertia further causes the cantilever tip to deflect through dry nitrogen. As a result, the positions of the two sides of the film relative to the dry nitrogen have swapped, that is, the initially back surface is facing dry nitrogen, and the surface initially facing dry nitrogen is facing air in the current state. Consequently, the direction of the film shrinkage is reversed, establishing a feedback loop of upstroke and downstroke. (Supplementary Movie S4).

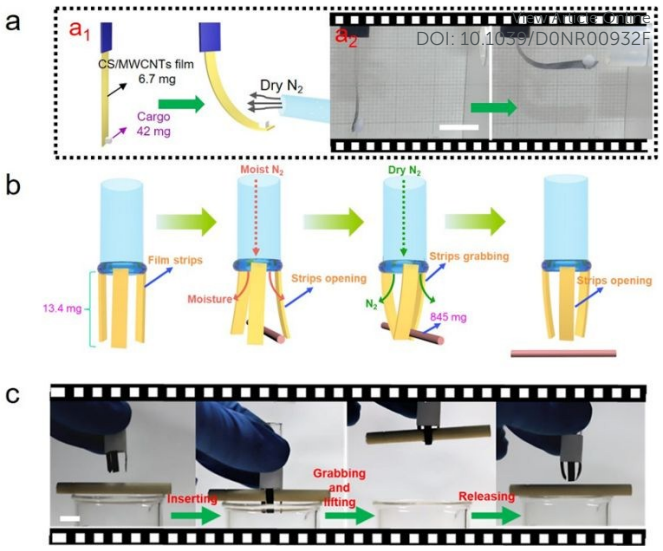

Fig. 4 (a_1): Schematic illustration of the lifting actuation as the cantilever cranes under stimulus; (a_2) optical images showing the smart cantilever craning to lift the cargo upon the dry stimulus; (b): Schematic illustration of the gripping device under dry and wet stimulus; (c): a series of optical images showing the smart device grabs, moves, and lays down a cargo due to the stimulus (Scale bar: 1 cm).

A hanged strip of CS/MWCNTs affixed at their upper terminus that respond to non-uniform exposure to stimulus by reversible bending can function as a cantilever crane, which harvests energy of the chemical potential contained within the humidity to convert it to mechanical work (Supplementary Movie S5). A 6.7 mg, 40-μm-thick strip of CS/MWCNTs was capable of hoisting a cargo of 28 mg (moist stimulus), 42 mg (dry stimulus) to a height of 2 cm (moist stimulus), 1.5 cm (dry stimulus) with largest tip deflection in 6 s (Fig. 4a). The work output and power density of this actuator are 0.84 J kg^{-1} and 0.14 W kg^{-1}(moist stimulus), and (1.3 J kg^{-1} and 0.22 W kg^{-1}) (dry stimulus).

Thanks to the different responses of the film to moist and dry stimulus, we can use both sources for the cooperative control of the bi-directional bending motion of composite film to achieve more complex movement. As shown in Fig. 4b, three composite film strips are glued to the outside of the glass tube to form a three-claw gripping device. As shown in Fig. 4c and Movie S6, when moist nitrogen passes, the three claws bend outward. When the clip model was placed on a cylindrical cargo, the three claws gather after dry nitrogen gas passing through the glass tube. The closed claw will grip and lift the object. After the removal of the dry nitrogen, the claws are open and the object can be laid down. By using this gripping device, we can transfer cargoes 63 times heavier than that of three strips. Based on this design, we can apply composite film in the system of soft robots driven by both moist and dry stimulus simultaneously.

View Article Online
DOI: 10.1039/D0NR00932F

Published on 24 February 2020. Downloaded by University of Leeds on 2/27/2020 8:47:54 PM.

Nanoscale Accepted Manuscript

Please do not adjust margins

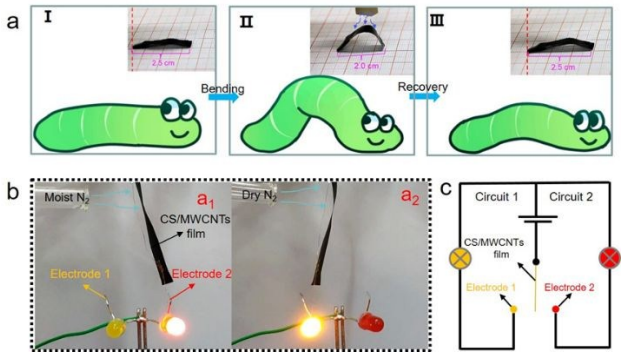

Fig. 5 (a): Motion of the device triggered by moist stimulus; (b): Photographs of the film as a bidirectional sensor which was assembled by a film coated with copper wire and two LED lights of different colors; (c): Diagram showing the experimental setup of parallel circuits.

Impressively, the CS/MWCNTs strip possessing high sensitivity and rapid response to stimulus can be utilized in smart motion device and bi-responsive detectors. A design has been developed to achieve linear locomotion of the actuator in response to temporal change of environmental humidity. The strip rides up first due to the moist stimulus, and moves forward due to the recovery by terminating the stimulus, as shown in Fig. 5a. Movie S7 shows this actuation system creeping or crawling under varying humidity.

We also constructed a device with a bidirectional actuation consisting of the CS/MWCNTs strip assembled with copper wire and two light-emitting diode (LED) lights with different colors (Fig. 5b). Fig. 5c shows a circuit diagram of the experimental setup containing two circuits (circuit 1 and 2) which are stimulated by moist and dry source. The initial states of both electrical circuits were open, and then the film bent away from moist source, which resulted in the closing of circuit 2 and the illumination of the red LED. When the strip was stimulated by a dry source from the same side, circuit 1 containing a yellow LED was closed. Upon the removal of the stimuli, the film recovered to a flat state and the LED was turned off. Consequently, the CS/MWCNTs 50 *wt*% strip acted as a bi-responsive single-pole double throw switch (Movie S8).

Conclusions

In conclusion, a bidirectional hygroresponsive actuator has been achieved from CS/MWCNTs film by virtue of the in-situ formation of bi-layer structure through inhomogeneous swelling/shrinking process owing to CNT-facilated water transport. The fabricated actuator exhibited outstanding and rapid actuation behaviors, which can be readily and effectively manipulated by varying the relative humidity difference and actuator chemical composition. The film displayed remarkable shape reconfiguration (including reversible bending, continual flipping, and oscillating) and demonstrated potential applications, such as lifting and transporting cargo. Furthermore, the composite film can be utilized to construct a smart motion device, and a touchless electronic device which outputs different signals in response to humid and dry stimulus. The actuation system developed here would be of particular uses for remotely controlling the devices in the difficult-to-access areas in a contactless mode, taking advantage of the fluctuations in the environmental humidity.

View Article Online DOI: 10.1039/D0NR00932F

Conflicts of interest

There are no conflicts to declare

Acknowledgements

The authors would like to thank the following for financial support: National Natural Science Foundation of China (No. 21104050), a project funded by the Priority Academic Program Development of Jiangsu Higher Education Institutions (PAPD), the fund (2017002) from the Key Laboratory of Advanced Textile Materials and Manufacturing Technology (Zhejiang Sci-Tech University), the Ministry of Education, State Key Laboratory of Pollution Control and Resource Reuse Fund(PCRRF18040), the Fundamental Research Funds and Welcome ISSF Junior Investigator Development Fellowship.

References

1 M. R. Islam, X. Li, K. Smyth, M. J. Serpe, *Angew. Chem. Int. Ed. Engl*., 2013, **52**, 10330-10333.
2 M. Ma, L. Guo, D. G. Anderson, R. Langer, *Science,* 2013, **339**, 186 -189.
3 Z. Pei, Y. Yang, Q. Chen, E. M. Terentjev, Y. Wei, Y. Ji, *Nat Mater.,* 2014, **13**, 36.
4 L. Ionov, *Adv. Funct. Mater*., 2013, **23**, 4555-4570.
5 Q. Zhao, J. W. Dunlop, X. Qiu, F. Huang, Z. Zhang, J. Heyda, J. Dzubiella, M. Antonietti, J. Yuan, *Nat. Commun*., 2014, **5**, 4293.
6 A. Sidorenko, T. Krupenkin, A. Taylor, P. Fratzl, J. Aizenberg, *Science,* 2007, **315**, 487-490.
7 P. Fratzl, F. G. Barth, *Nature,* 2009, **462**, 442.
8 P. Chen, S. He, Y. Xu, X. Sun, H. Peng, *Adv. Mater.,* 2015, **27**, 4982-4988.
9 Q. Zhao, J. Heyda, J. Dzubiella, K. Tauber, J. W. Dunlop, J. Yuan, *Adv Mater.,* 2015, **27**, 2913-2917.
10 L. Zhang, P. Naumov, *Angew. Chem. Int. Ed. Engl.,* 2015, **54**, 8642-8647.
11 F. Zhou, W. Shu, M. E. Welland, W. T. Huck, *J. Am. Chem. Soc.,* 2006, **128**, 5326-5327.
12 W. Wu, L. Yao, T. Yang, R. Yin, F. Li, Y. Yu, *J. Am. Chem. Soc.,* 2011, **133**, 15810-15813.
13 M. Ji, N. Jiang, J. Chang, J. Sun, *Adv. Funct. Mater.,* 2014, **24**, 5412-5419.
14 H. Arazoe, D. Miyajima, K. Akaike, F. Araoka, E. Sato, T. Hikima, M. Kawamoto, T. Aida, *Nat. Mater*., 2016, **15**, 1084.
15 M. Wang, X. L. Tian, R. H. A. Ras, O. Ikkala, *Adv. Mater. Interfaces*, 2015, **2**, 7.
16 Q. Zhu, Y. X. Jin, W. Wang, G. Sun, D. Wang, *ACS Appl. Mater. Interfaces*, 2019, **11**, 1440.
17 M. M. Ma, L. Guo, D. G. Anderson, R. Langer, *Science*, 2013, **339**, 186.
18 H. Cheng, F. Zhao, J. Xue, G. Shi, L. Jiang, L. Qu, *ACS Nano*., 2016, **10**, 9529.
19 J. He, P. Xiao, J. Zhang, Z. Liu, W. Wang, L. Qu, Q. Ouyang, X. Wang, Y. Chen, T. Chen, *Adv. Mater. Interfaces*, 2016, **3**, 1600169.

Published on 24 February 2020. Downloaded by University of Leeds on 2/27/2020 8:47:54 PM.

Nanoscale Accepted Manuscript

This journal is © The Royal Society of Chemistry 20xx

Please do not adjust margins

20 T. J. Jia, Y. Wang, Y. Y. Dou, Y. W. Li, M. J. de Andrade, R. Wang, S. L. Fang, J. J. Li, Z. Yu, R. Qiao, Z. J. Liu, Y. Cheng, Y. W. Su, M. Minary-Jolandan, R. H. Baughman, D. Qian, Z. F. Liu, *Adv. Funct. Mater*., 2019, **29**, 12.
21 Y. Ma, Y. Zhang, B. Wu, W. Sun, Z. Li, J. Sun, *Angew Chem. Int. Ed*., 2011, **50**, 6254.
22 M. Dai, O. T. Picot, J. M. Verjans, L. T. de Haan, A. P. Schenning, T. Peijs, C. W. Bastiaansen, *ACS Appl. Mater. Interfaces*, 2013, **5**, 4945.
23 T. Wu, M. Frydrych, K. O'Kelly, B. Chen, *Biomacromolecules*, 2014, **15**, 2663.
24 J. K. Mu, G. Wang, H. P. Yan, H. Y. Li, X. M. Wang, E. L. Gao, C. Y. Hou, A. T. C. Pham, L. J. Wu, Q. H. Zhang, Y. G. Li, Z. P. Xu, Y. Guo, E. Reichmanis, H. Z. Wang, M. F. Zhu, *Nat. Commun*., 2018, **9**, 10.
25 W. Wang, C.X. Xiang, Q.Z. Liu, M.F. Li, W.B. Zhong, Kelu Yana, D. Wang, *J. Mater. Chem. A*, 2018, **6**, 22599–22608.
26 M. Wang, X. Tian, R. H. A. Ras, O. Ikkala, *Adv. Mater. Interfaces*, 2015, **2**, 1500080.
27 S. Douezan, M. Wyart, F. Brochard-Wyart, D. Cuvelier, *Soft. Matter.,* 2011, **7**, 1506-1511.
28 E. Reyssat, L. Mahadevan, *EPL*., 2011, **93**, 54001.
29 Y. Ge, R. Cao, S. Ye, Z. Chen, Z. Zhu, Y. Tu, D. Ge, X. Yang, *Chem. Commun*., 2018. **255**, 3979-3982.
30 B. E. Treml, R. N. McKenzie, P. Buskohl, D. Wang, M. Kuhn, L. S. Tan, R. A. Vaia, *Adv. Mater*., 2018, **30**, 1870046.
31 J. Mu, G. Wang, H. Yan, H. Li, X. Wang, E. Gao, C. Hou, A. T. C. Pham, L. Wu, Q. Zhang, Y. Li, Z. Xu, Y. Guo, E. Reichmanis, H. Wang, M. Zhu, *Nat. Commun*., 2018, **9**, 590.
32 J. G. Deng, Y. You, H. Bustamante, V. Sahajwalla, R. K. Joshi, *Chem. Sci*., 2017, **8**, 1701-1704.
33 H. B. Huang, Z. G. Song, N. Wei, L. Shi, Y. Y. Mao, Y. L. Ying, L. W. Sun, Z. P. Xu, X. S. Peng, *Nat. Commn*., 2013, **4**, 2979.
34 G. Algara-Siller, O. Lehtinen, F. C. Wang, R. R. Nair, U. Kaiser, H. A. Wu, A. K. Geim, I. V. Grigorieva, *Nature*, 2015, **519**, 443–445.
35 Alberto Striolo, *Nano Lett*., 2006, **6**, 633–639.
36 M. Tichy, R. Zahradnik, *J. Phys. Chem. C*., 1969, **73**, 534-544.
37 J. Duan, X. Liang, J. Guo, K. Zhu, L. Zhang, *Adv. Mater*., 2016, **28**, 8037-8044.
38 T.-D. Nguyen, B. U. Peres, R. M. Carvalho, M. J. MacLachlan, *Adv. Funct. Mater*., 2016, **26**, 2875-2881.
39 J. H. Jeon, R. K. Cheedarala, C.-D. Kee, I. K. Oh, *Adv. Funct. Mater*., 2013, **23**, 6007-6018.
40 A.I. Skoulidas, D.M. Ackerman, J.K. Johnson, D.S. Sholl, *Phys. Rev. Lett*., 2002, 89.
41 H.B. Chen, J.K. Johnson, D.S. Sholl, *J. Phys. Chem. B*, 2006, **110**, 1971–1975.
42 H.B. Chen, D.S. Sholl, *J. Membrane Sci*., 2006, **269**, 152–160.
43 B.J. Hinds, N. Chopra, T. Rantell, R. Andrews, V. Gavalas, L.G. Bachas, *Science*, 2004, **303**, 62–65.
44 S. Joseph, N.R. Aluru, *Nano Lett*., 2008, **8**, 452–458.
45 A. Kalra, S. Garde, G. Hummer, *Proc. Natl. Acad. Sci. U.S.A*., 2003, **100**, 10175–10180.
46 M. Majumder, N. Chopra, R. Andrews, B. J. Hinds, *Nature*, 2005, **438**, 44.
47 S. Kim, L. Chen, J.K. Johnson, E. Marand, *J. Membrane Sci*., 2007, **294**, 147–158.
48 X.F. Wang, X.M. Chen, K. Yoon, D.F. Fang, B.S. Hsiao, B. Chu, *Environ. Sci. Technol*., 2005, **39**, 7684–7691.
49 B. Mi, *Science*, 2014, **343**, 740–742.
50 R. R. Nair, H. A. Wu, P. N. Jayaram, I. V. Grigorieva, A. K. Geim, *Science*, 2012, **335**, 442–444.
51 S. F. Wang, L. Shen, W. D. Zhang, Y. J. Tong, *Biomacromolecules*, 2005, **6**, 3067-3072.
52 N. J. W. Reuvers, H. P. Huinink, H. R. Fischer, O. C. Adan, *Macromolecules*, 2012, **45**, 1937-1945.

View Article Online
DOI: 10.1039/D0NR00932F

Published on 24 February 2020. Downloaded by University of Leeds on 2/27/2020 8:47:54 PM.

Nanoscale Accepted Manuscript